

## NOTICE

This report was prepared as an account of work sponsored by the United States Government. Neither the United States nor the United States Atomic Energy Commission, nor any of their employees, nor any of their contractors, subcontractors, or their employees, makes any warranty, express or implied, or assumes any legal liability or responsibility for the accuracy, completeness or usefulness of any information, apparatus, product or process disclosed, or represents that its use would not infringe privately owned rights.

## EXPERIMENTAL FISSION BARRIERS FOR ACTINIDE NUCLEI\*

B.B. Back<sup>†</sup>, H.C. Britt<sup>††</sup>, J.D. Garrett<sup>†††</sup>,  
Ole Hansen<sup>††††</sup> and B. Leroux<sup>†††††</sup>

Los Alamos Scientific Laboratory, USA; Nuclear Structure Research Laboratory, University of Rochester, USA; Brookhaven National Laboratory, USA; and University of Bordeaux, FRANCE

## ABSTRACT

Fission probability distributions are measured for a number of isotopes of Th, Pa, U, Np, Pu, Am, Cm and Bk using (d,pf), (t,pf), (<sup>3</sup>He,df), (p,p'f), (<sup>3</sup>He,αf) and (t,αf) reactions. The results along with previous data available from (d,pf) and (n,f) studies are analyzed with a statistical model and estimates are obtained for the heights,  $E_A$  and  $E_B$ , and curvatures,  $\hbar\omega_A$  and  $\hbar\omega_B$ , of the two peaks of the fission barrier for a wide range of actinide nuclei. The statistical model used for the analysis of odd A and odd-odd nuclei includes competition between fission, neutron emission and gamma ray de-excitation in the decay of the compound nucleus. The results suggest that fission widths which are greater by about a factor of 4 than those calculated are necessary to reproduce the magnitude of the measured fission probabilities. The results show that  $E_A$  is roughly constant throughout this region and  $E_B$  decreases

\*Work supported by the U.S. Atomic Energy Commission

<sup>†</sup>Permanent address: Niels Bohr Institute, Denmark; supported by Staten naturvidenskabelige forskningsråd, Denmark

<sup>††</sup>Presently at Nuclear Structure Research Laboratory, University of Rochester; Permanent address: Los Alamos Scientific Laboratory

<sup>†††</sup>Permanent address: Brookhaven National Laboratory, USA

<sup>††††</sup>Permanent address: Niels Bohr Institute, Denmark

<sup>†††††</sup>Permanent address: University of Bordeaux, France

DISTRIBUTION OF THIS DOCUMENT IS UNLIMITED

MASTER

with increasing  $Z$ . An exception to the approximate constancy of  $E_A$  is in Cm where  $E_A$  drops by 1.0 MeV from  $^{248}\text{Cm}$  to  $^{250}\text{Cm}$ . In some cases an odd-even fluctuation of 0.30-0.50 MeV is observed in the experimental  $E_A$  values.

## EXPERIMENTAL FISSION BARRIERS FOR ACTINIDE NUCLEI\*

B.B. Back<sup>†</sup>, H.C. Britt<sup>††</sup>, J.D. Garrett<sup>†††</sup>,  
 Ole Hansen<sup>††††</sup> and B. Leroux<sup>†††††</sup>

Los Alamos Scientific Laboratory, USA; Nuclear Structure  
 Research Laboratory, University of Rochester, USA; Brookhaven  
 National Laboratory, USA; and University of Bordeaux, FRANCE

## 1. INTRODUCTION

At the last IAEA conference on the Physics and Chemistry of Fission<sup>[1]</sup> in 1969 many of the exciting new developments were related to the investigation of the qualitative implications of the effects of deformed nuclear shells on the potential energy surfaces associated with the fission process and the wide variety of experiments that had recently confirmed the major predictions of this new theory. At that conference experimental results were presented on the existence of fission isomers in a wide range of actinide nuclei, intermediate structure resonances in subbarrier neutron fission, and gross structure resonances in (n,f) and (d,pf) studies. All of these experimental phenomena were found to be consistent with the concept of a two peaked fission barrier that resulted theoretically from fluctuations in the shell corrections to the single peaked fission barrier predicted by the liquid drop model.

\*Work supported by the U.S. Atomic Energy Commission

<sup>†</sup>Permanent address: Niels Bohr Institute, Denmark;  
 supported by Staten naturvidenskabelige forskningsråd,  
 Denmark

<sup>††</sup>Presently at Nuclear Structure Research Laboratory,  
 University of Rochester; Permanent address: Los Alamos  
 Scientific Laboratory

<sup>†††</sup>Permanent address: Brookhaven National Laboratory, USA

<sup>††††</sup>Permanent address: Niels Bohr Institute, Denmark

<sup>†††††</sup>Permanent address: University of Bordeaux, France

Since the last conference there has been considerable activity both theoretically and experimentally directed toward trying to quantitatively determine the characteristics of the potential energy surface involved in fission and to try to understand how these complex potential energy surfaces affect some aspects of the fission process. In subsequent papers at this conference both the current status of potential energy calculations and recent theoretical efforts to qualitatively understand the more difficult problems of fission dynamics will be reviewed<sup>[2,3]</sup>. In our paper we will present a review of current efforts to try to experimentally determine fission barrier characteristics for actinide elements with particular emphasis on recent direct reaction fission results from Los Alamos. In general, the fission barrier properties that can be most readily compared with theoretical calculations are the energies of the two saddle points and the secondary minimum relative to the ground state. We will concentrate on these properties although in some cases the experiments also yield information on barrier curvatures.

Figure 1 illustrates schematically the two types of experiment which have been used to obtain most of the current information on fission barrier heights. In a direct reaction fission experiment a direct reaction (or neutron capture reaction) is used to produce a residual nucleus at a particular excitation energy and the branching ratio for decay by fission relative to neutron or gamma deexcitation (or the fission cross section) is measured. This type of experiment gives information primarily on the height and curvature of the highest peak in the fission barrier. However, in some cases resonances are observed which can be associated with vibrations near the top of the second well and a detailed analysis of the experimental results gives information on both peaks. The results and analysis for even-even fissioning nuclei where these resonance structures are observed will be presented in the following paper<sup>[4]</sup>. Figure 1 also illustrates schematically the population of a shape isomeric state in the second well following the evaporation of a neutron. In most cases of experimental interest the isomeric states are populated following the subsequent evaporation of two or three neutrons but qualitatively the data analysis is the same<sup>[5]</sup>. In practice fission isomer excitation functions have been analyzed using  $E_A$  values from other sources and the experimental data is used to determine  $E_B$  and  $E_{II}$ . Thus, in the heavy actinides where  $E_A > E_B$  the direct-reaction fission and the fission isomer excitation function measurements are complementary. In addition, intermediate structure resonances from subbarrier neutron fission experiments can in some cases be used to estimate  $E_{II}$ <sup>[5,6]</sup>. Finally, the half-lives for fission decay from the ground and isomeric states give information on the curvatures and/or average mass parameters and these aspects will be discussed in other contributions at this conference.

The actinide nuclei which have been studied either by direct-reaction fission or fission isomer techniques are indicated in Figure 2. It is seen that the current direct-reaction fission results plus earlier (d,pf) [7] and (n,f) [8] results provide a rather extensive survey of the actinide region. For several plutonium, americium and curium isotopes complementary information is available from both types of experiment.

In the current direct-reaction fission studies a variety of reactions including (d,p), (t,p), ( $^3\text{He,d}$ ), (p,p'), ( $^3\text{He,\alpha}$ ) and (t, $\alpha$ ) have been used so that a large number of fissioning nuclei could be investigated starting from the limited number of available target species. Of particular interest is the ( $^3\text{He,df}$ ) reaction which allows the investigation of many odd Z nuclei starting from the relatively plentiful even Z targets. In general, it was found that cross sections for exciting nuclei to energies near the top of the fission barrier were quite adequate for (d,p), (t,p) and ( $^3\text{He,d}$ ) reactions but the other reactions tried were of limited usefulness.

In the remainder of this paper we will present:

- 1) some of the general features of the experimental setup and results, 2) a discussion of techniques used to analyze the data for odd A and odd-odd residual nuclei and 3) a survey of the experimental information currently available on the barrier heights  $E_A$  and  $E_B$  for actinide elements. A discussion of resonance phenomena and the analysis of data from even-even fissioning nuclei will be given in the following paper.

## 2. EXPERIMENTAL RESULTS

The setup used in the direct-reaction fission studies is illustrated schematically in Fig. 3. The outgoing reaction particle is identified and its energy measured with a resolution of 40-100 keV in a standard  $\Delta E$ -E counter telescope placed at an angle near  $90^\circ$ . For each event the excitation energy of the residual nucleus can be determined from the kinetic energy of the outgoing reaction particle. In the experiment the spectrum of reaction particles are measured both in a configuration where a coincidence is required with a large annular fission detector (coincidence spectrum) and in a configuration where no coincidence is required (singles spectrum). Using a measured solid angle for the fission detector and assuming that the coincident fission fragments are isotropically distributed the ratio of coincidence to singles spectra can be transformed to a distribution of fission probability as a function of excitation energy in the residual nucleus. The absolute energy scales are determined from known Q values [9] and a calibration of the counter telescope with known energy lines [10] from appropriate reactions on lead targets. Absolute excitation energies determined in this manner are believed to be accurate to  $\pm 50$  keV. Systematic errors

in the absolute fission probabilities are believed to be less than  $\pm 20\%$  for ( $^3\text{He}, \text{df}$ ) cases,  $< \pm 30\%$  for ( $t, \text{pf}$ ) cases, and  $< \pm 40\%$  for ( $t, \alpha\text{f}$ ), ( $^3\text{He}, \alpha\text{f}$ ) and ( $p, p'\text{f}$ ) cases. For ( $d, \text{pf}$ ) reactions to excitation energies above the neutron binding energy systematic uncertainties in the fission probabilities are estimated to be less than  $\pm 30\%$  with part of this estimate being due to uncertainties in the corrections for protons coming from deuteron breakup reactions. The targets used in this experiment were all oxides vacuum evaporated on carbon backings. This experimental setup is similar to previous experiments [7, 11] and will be described in detail in a more comprehensive report on these results [12].

Typical coincidence and singles spectra are shown in Figs 4 and 5. In the ( $t, \text{pf}$ ) reactions the peaks come from reactions on carbon and oxygen in the target and the solid lines represent extrapolated estimates of the singles counting rate from the actinide element. For  $^3\text{He}$  reactions the  $Q$  values and kinematics are such that light element contaminants do not appear in this excitation energy range at  $90^\circ$ . The absence of light element contamination in the singles spectrum for ( $^3\text{He}, \text{d}$ ) reactions allows a more reliable determination of the fission probability distribution for these cases. The singles spectra have been normalized to show the magnitude of the accidental corrections in the coincidence measurements. It is seen that in most cases the accidental corrections are negligible. For ( $t, \text{pf}$ ) and ( $d, \text{pf}$ ) reactions the angle of the proton detector was varied in the range  $70^\circ$ - $100^\circ$  in order to minimize the accidental contributions in the threshold region.

The results for typical even-even nuclei (fig.4) show pronounced resonance structure characteristic of the sub-barrier resonant penetration of the two peaks of the fission barrier. These resonances come from the enhanced fission penetrability when the excitation energy overlaps the energy of a vibrational state in the second well. The general characteristics of these resonances will be discussed in the next paper [4]. In contrast the odd  $A$  and odd-odd nuclei (fig.5) do not show subbarrier resonant structure which we interpret as being due to increased mixing (or damping) of the vibrational states in the second well with other types of compound excitations. The damping for the odd nuclei is expected to be greater than for even-even nuclei because of the increased density of compound levels in well II at the top of the barrier.

Previous comparisons [13] of ( $t, \text{pf}$ ), ( $d, \text{pf}$ ) and ( $n, \text{f}$ ) reactions to the same residual nuclei have shown that for excitation energies above the neutron binding energy a significant fraction of the singles protons from ( $d, \text{p}$ ) reactions come from breakup of the deuteron without the corresponding excitation of the residual nucleus. This effect leads to low estimates for the fission probabilities from ( $d, \text{pf}$ ) reactions for energies above the neutron binding energy. In the current analysis of experimental data we have corrected all ( $d, \text{pf}$ ) fission probabilities by multiplying by a function of  $(E^* - B_n)$  taken from Britt and Cramer [13].

### 3. STATISTICAL MODEL FOR ANALYSIS OF EXPERIMENTAL RESULTS

From the experimental results it is seen that there are significant differences in the requirements for a statistical model which will reproduce the results from direct reaction fission experiments involving even-even residual nuclei and those involving odd A or odd-odd nuclei. In particular the even-even nuclei show resonant penetration of the two barriers but to help in simplifying the problem only a few vibrational and rotational excitations are involved in the fission penetrability near threshold. The excitation energies of these vibrations can be estimated from previous angular correlation measurements<sup>[11]</sup>. In addition, the fission thresholds for even-even actinide nuclei are usually well below the neutron binding energy so that in the region of most interest only fission and gamma ray deexcitation can compete.

For the odd nuclei since in most cases resonances are not observed in the fission probability distributions, the complete damping approximation which considers the penetration of the two barriers separately can be used. However, for odd nuclei the competition from neutron emission as well as gamma decay must be included and estimates of the fission penetrabilities involve summations over distributions of transition states about which there is no experimental information.

The different requirements of the two cases have led us to develop two rather different statistical models. The model used to fit the even-even nuclei will be discussed in the following talk<sup>[4]</sup>. The model used to describe the fission of odd A and odd-odd residual nuclei is detailed below in general terms and will be described in quantitative detail in a subsequent more comprehensive paper<sup>[14]</sup>.

The statistical model we have used to describe the fission of odd residual nuclei is shown diagrammatically in Fig. 6. The transmission coefficients  $T_f$  are calculated in the complete damping limit where the transmission through the two peaks are treated separately. In this limit:

$$T_f = \frac{T_A \cdot T_B}{T_A + T_B} \cdot f\left(\frac{W_{II}}{D_{II}}\right)$$

where  $f$  is a correction factor that takes into account the finite width of the compound levels in the second minimum through which the fission is coupled. If the levels in the second well are assumed to be equispaced then it can be shown<sup>[12]</sup> that the fission probability is given by

$$P_f = (1 + a^2 + 2a \coth(t/2))^{-1/2}$$

where

$$a = (T_\gamma + T_n) \cdot (T_A + T_B) / (T_A \cdot T_B)$$

and

$$t = 4\pi W_{II}/D_{II} = T_A + T_B.$$

In the limit where  $t \gg 1$  (i.e. levels in second well strongly overlap) this expression reduces to the more usual expression:

$$P_f = \frac{T_f}{T_f + T_n + T_\gamma}$$

where

$$T_f = T_A \cdot T_B / (T_A + T_B).$$

The calculation of the fission probability now reduces to a calculation of the transmission coefficients  $T_A$ ,  $T_B$ ,  $T_n$ , and  $T_\gamma$ . The calculation of these transmission coefficients involves estimating the distribution of residual levels available for neutron and gamma deexcitation and the distribution of saddle point transition states for  $T_A$  and  $T_B$ . At the deformation of the first well, ( $T_n$  and  $T_\gamma$  calculations) the residual levels were assumed to be discrete for excitation energies less than 1 MeV and a continuous level density was used for excitation energies greater than 1 MeV. For odd-odd nuclei a continuous level density was used at all energies. The continuous level density was obtained from calculated single particle levels as described previously<sup>[5]</sup>. For odd A nuclei the discrete levels were taken as rotational bands build on the one quasi-particle states obtained from calculated single particle levels<sup>[5,15,16]</sup> with the appropriate shifts due to pairing. For even-even nuclei the discrete levels were obtained from a composite spectrum based on experimental measurements in the uranium-curium region. Then  $T_\gamma$  and  $T_n$  were estimated from expressions given previously<sup>[5]</sup> except that optical model transmission coefficients were used in the  $T_n$  calculations. The  $T_\gamma$  values were normalized so that calculated values of  $T_\gamma$  reproduce measured values at the neutron binding energy for odd Pu isotopes.

The level spectra used in the  $T_A$  and  $T_B$  calculations were obtained in a similar manner except that single particle levels appropriate to the first saddle and second asymmetric saddle were used. The transmission coefficients were calculated as a sum of penetrabilities through parabolic barriers with curvatures  $\hbar\omega_A$  and  $\hbar\omega_B$ .

The level spectra used in these calculations are shown in fig. 7 where solid lines indicate energy regions where continuous level densities were used and the triangles represent the average total density of the discrete levels for a given case. At the first saddle discrete levels from Bosterli et al<sup>[15]</sup> and Tsang<sup>[16]</sup> are compared and it is seen that the average densities are similar. Figure 8 shows that below 1 MeV the continuous level density calculation seriously underestimates the total number of levels. This discrepancy is due to the inadequacy at low excitation energies of the saddle point approximation<sup>[5]</sup> used in estimating the continuous level density.

Figure 8 compares the density of calculated one quasiparticle states with the continuous level density for  $^{241}\text{Pu}$ . The continuous level density is normalized to the measured value for  $1/2^+$  states at the neutron binding energy. Also shown in fig. 8 are the density of measured levels<sup>[17]</sup>



for  $^{235}\text{U}$  and it is seen that the calculated density of one quasiparticle states is in reasonable agreement with measurements.

#### 4. FITS TO EXPERIMENTAL RESULTS

Using the statistical model described in the previous section experimental fission probability distributions for odd A and odd-odd nuclei were fit in order to systematically determine properties of the fission barrier for actinide nuclei. In these fits different procedures were used for nuclei in the region Pu-Bk and for the Pa-Np region.

As we pointed out in the introduction for many isotopes of Pu, Am and Cm there is considerable data available from fission isomer studies which can be used to estimate  $E_{\text{II}}$ ,  $E_{\text{B}}$  and  $\hbar\omega_{\text{B}}$ . Therefore, in fitting the direct reaction fission data in this region we have fixed  $E_{\text{B}}$  and  $\hbar\omega_{\text{B}}$  to the values determined from fission isomer studies or in cases where no data is available to values that were extrapolated from nearby nuclei. The experimental data were then fit by varying  $E_{\text{A}}$ ,  $\hbar\omega_{\text{A}}$  and a normalization factor to get the correct plateau value for the fission probability. For the odd Pu and Cm isotopes and the odd-odd Am isotopes this normalization factor was an adjustable constant ( $G_{\text{n}}$ ) multiplying the function  $\Gamma_{\text{n}}/\Gamma_{\text{f}}$ . For the odd Am isotopes where the fission threshold is below the neutron binding energy the adjustable constant ( $G_{\text{v}}$ ) multiplied  $\Gamma_{\text{v}}/\Gamma_{\text{f}}$ . In addition to the results obtained in the present experiment, data from previous (d,pf) [7] and (n,f) [6,18] studies were also fit to obtain a consistent set of barriers. The published (n,f) cross sections were converted to fission probabilities as described previously [13]. The fits obtained to the experimental data are shown in Figures 9 and 10. It is seen that using the three adjustable parameters the shapes of the distributions can be reasonably well reproduced near threshold but at energies above the peak  $P_{\text{f}}$  value the calculations from odd A nuclei decrease sharply whereas the data show a plateau. This result indicates that the functional form for  $\Gamma_{\text{n}}/\Gamma_{\text{f}}$  obtained from the present statistical model is not adequate. This point will be discussed in more detail in the next section.

For the Pa and Np nuclei there is no independent information available (e.g. from fission isomers) so that the parameters  $E_{\text{A}}$ ,  $\hbar\omega_{\text{A}}$ ,  $E_{\text{B}}$ ,  $\hbar\omega_{\text{B}}$ , and the normalization factors  $G_{\text{n}}$ , or  $G_{\text{v}}$  are all unknown. In general, fits to the experimental fission probability distributions were not capable of uniquely determining all of these parameters. Therefore, the experimental results were fit by fixing  $\hbar\omega_{\text{A}}$  and  $\hbar\omega_{\text{B}}$  to average values determined from the heavier nuclei and then varying  $E_{\text{A}}$ ,  $E_{\text{B}}$ , and  $G_{\text{n}}$  or  $G_{\text{v}}$ . In most cases  $G_{\text{n}}$  values were held fixed to average values determined from the Pu-Bk results. In addition to the Pa and Np results fission probabilities obtained [13] from (n,f) cross sections for  $^{235}\text{U}$ ,  $^{237}\text{U}$  and  $^{239}\text{U}$  were also analyzed. Due to the lack of independent information on  $E_{\text{B}}$  and  $\hbar\omega_{\text{B}}$  and because  $E_{\text{A}} \approx E_{\text{B}}$

the uncertainties on the barrier parameters determined for the Pa-Np region are greater than for the Pu-Bk nuclei. The results of these fits are shown in Figure 11. For  $^{231}\text{Pa}$  and  $^{232}\text{Pa}$  there appears to be some resonant structure which can not be reproduced in the complete damping approximation used in our statistical model. This resonant structure may be analogous to the more pronounced structure observed in  $^{231}\text{Th}$ .

The barrier parameters obtained from analysis of all the odd nuclei are given in Table I. Results for even-even nuclei are tabulated in the following paper<sup>[4]</sup>.

## 5. EXPERIMENTAL VS CALCULATED DECAY WIDTHS

Within the context of the statistical model described in Section III the widths for neutron and fission decay are calculated on an absolute basis and the adjustable normalization in the gamma decay width was fixed by normalizing to experimental data. Therefore, it was initially expected that the normalization factors  $G_n$  and  $G_\gamma$  should each be equal to 1 except for fluctuations due to systematic uncertainties in the absolute experimental fission probabilities. The results from the fits indicate that this is not the case as is shown in Fig. 12.

Except for  $^{249}\text{Cm}$  the values of  $G_\gamma$  are generally consistent with 1 although the Am and Bk nuclei are better fit with a value of  $\sim 2$  and the Pa and Np isotopes (Table I) show a preference for values of 3-4. In contrast the  $G_n$  values are definitely not consistent with 1 and a value of  $G_n = 0.2-0.3$  gives the best average representation of all the results. Furthermore, the underestimates of the fission probabilities at high energies with the current statistical model suggests that the value of  $G_n$  is even less at energies of 1-2 MeV above the fission threshold.

The  $\Gamma_n$  and  $\Gamma_f$  calculations involve only an estimate of the spectrum of states available for de-excitation in the first well ( $\Gamma_n$ ) and across the two saddle points ( $\Gamma_f$ ). For nuclei in the region Pu-Bk the transmission across the first saddle point is of major importance in estimating  $\Gamma_f$ . Since average properties of the level spectra involved in the  $\Gamma_n$  calculation can be checked against experiment at low energy and the continuous level densities are normalized to experimental values at high energies it seems most reasonable to connect the low values of  $G_n$  with an underestimate of  $\Gamma_f$ . By using a single normalization factor for all the high energy level densities and treating the discrete levels in similar ways at the first minimum and the saddle points we have effectively assumed that the enhancement of the level densities due to coupling with low-lying collective excitations is the same at the minima and the saddle points. The low and possibly energy dependent value we obtain for  $G_n$  may indicate that the level densities at the saddle points are enhanced by coupling to additional low-lying collective excitations. The theoretical justification for such an

effect will be discussed in detail in other contributions to this conference [19,20].

This connection of low  $G_n$  values with an underestimate of the level density at the saddle point is, however, not consistent with the higher values obtained for  $G_\gamma$ . If the  $\Gamma_n$  and  $\Gamma_\gamma$  calculations are correct and the main difficulty is in calculating  $\Gamma_f$  then  $G_n$  and  $G_\gamma$  should be roughly equal and this is not the case. Therefore, it appears that there are still unsolved problems in the attempts to calculate relative values of  $\Gamma_f$ ,  $\Gamma_n$ ,  $\Gamma_\gamma$ .

## 6. EXPERIMENTAL FISSION BARRIERS

The barrier heights  $E_A$  and  $E_B$  extracted from the experimental data for Pu-Bk isotopes are shown in Fig. 13. Figure 13 includes results from the analysis of odd A and odd-odd nuclei as described earlier in this paper, results from the analysis of data from even-even nuclei described in the following paper [4] and estimates of  $E_B$  from the analysis of fission isomer excitation functions [5]. For the two cases where there is overlap,  $^{238}\text{Pu}$  and  $^{240}\text{Pu}$ , the  $E_B$  values estimated from the analysis of fission isomer data agree well with values obtained from these direct reaction fission experiments.

In the discussion below we will concentrate on some of the general trends for the barrier heights in actinide nuclei and in a later paper [2] at this conference these barrier heights will be compared with various theoretical predictions.

The outstanding characteristics of the fission barriers for nuclei in the Pu-Bk region are:

1. The values for  $E_A$  show a decrease with increasing neutron number but do not seem to vary significantly with proton number. This trend is contrary to most theoretical calculations which show  $E_A$  increasing with proton number.
2. The values of  $E_B$  do not seem to show a consistent trend with neutron number but decrease strongly with increasing proton number. These trends are qualitatively similar to theoretical predictions.
3. The  $E_A$  values for Pu and Am isotopes and possibly the  $E_B$  values for Am isotopes show an apparent odd-even fluctuation with  $E_A$  being 0.3-0.5 MeV higher for odd neutron than for even neutron nuclei. This result would be consistent with a larger pairing gap at the saddle point and can be compared to an average value  $\Delta_{\text{saddle}} - \Delta_{\text{ground state}} \approx 0.23$  MeV obtained from recent theoretical calculations [15] which assume that the pairing strength is independent of deformation. The apparent experimental odd-even fluctuations should be viewed with some caution, however, because the even N nuclei involve competition between fission and

gamma emission near threshold whereas the odd N nuclei have fission thresholds above the neutron binding energy. Therefore, systematic errors in the estimates of  $\Gamma_\gamma$  relative to  $\Gamma_n$  could lead to spurious odd-even effects. At present we believe that the  $\pm 0.2$  MeV uncertainties in  $E_A$  for these nuclei are realistic but as noted in the previous section the normalizations of the various decay widths are not completely understood.

4. The  $E_A$  values for Cm isotopes show a decrease of  $\sim 1.0$  MeV in going from  $^{248}\text{Cm}$  ( $N=152$ ) to  $^{250}\text{Cm}$  ( $N=154$ ). This decrease seems to be significantly greater than the additional binding of  $\sim 0.6$  MeV [21,22] attributed to the  $N = 152$  shell for the equilibrium shape of  $^{248}\text{Cm}$  and is not apparent in the  $E_B$  estimates. The results suggest that there is an additional decrease of  $\sim 0.4$  MeV in the binding at the first saddle point between  $^{248}\text{Cm}$  and  $^{250}\text{Cm}$  when measured relative to a liquid drop mass surface.

The experimental barrier parameters for Th-Np nuclei are shown in Fig. 14. The barrier parameters for  $^{231}\text{Th}$  are taken from reference 23. The uncertainties in the estimated barrier heights for odd A and odd-odd nuclei are somewhat greater than in the Pu-Bk region because of the lack of fission isomer results to tie down the  $E_B$  and  $\hbar\omega_B$  values. The results again show  $E_A$  relatively constant and  $E_B$  decreasing with increasing proton number. The dependence on neutron number and possible odd-even effects do not seem as prominent as for the Pu-Bk region but details are obscured by the larger uncertainties on the estimated barrier heights.

## 7. CONCLUSION

In this paper we have presented a summary of the new data from direct reaction fission experiments which when coupled with previous (d,pf) and (n,f) data and analyzed with a realistic statistical model lead to a self consistent set of fission barriers for a large number of actinide nuclei from Th ( $Z=90$ ) through Bk ( $Z=97$ ). These results along with systematic results from fission isomer studies form a set of experimental barriers which can be used to test current theoretical estimates of fission barrier properties. How well the theories stand the test of experiment will be shown in the theoretical chapter of this story in a later paper [2].

We are grateful to J. Lerner at Argonne National Laboratory for producing the  $^{248}\text{Cm}$  target. It is a pleasure to acknowledge useful discussions with S. Bjørnholm, A. Bohr, J.R. Huizenga, J.E. Lynn, B. Mottelson, S.G. Nilsson, J.R. Nix, and R. Vandenbosch. We would like to thank the Neutron Cross Section Group at Brookhaven National Laboratory for providing tabulations of current (n,f) cross section data for many of the isotopes of interest.

## REFERENCES

- [1] Proceedings of the Second International Atomic Energy Agency Symposium on Physics and Chemistry of Fission, Vienna, 1969 (International Atomic Energy Agency, Vienna, 1969).
- [2] J.R. NIX and P. MÖLLER, Paper IAEA/SM-174/202, this conference.
- [3] H.C. PAULI and T. LEDERGERBER, Paper IAEA/SM-174/206, this conference.
- [4] B.B. BACK, H.C. BRITT, J.D. GARRETT and OLE HANSEN, Paper IAEA/SM-174/27, this conference.
- [5] H.C. BRITT, M. BOLSTERLI, J.R. NIX and J.L. NORTON, Phys. Rev. C7(1973)801; H.C. BRITT, S.C. BURNETT, B.H. ERKKILA, J.E. LYNN and W.E. STEIN, Phys. Rev. C4(1971)1444.
- [6] G.F. AUCHAMPAUGH, J.A. FARRELL and D.W. BERGEN, Nucl. Phys. A171(1971)31.
- [7] B.B. BACK, J.P. BONDORF, G.A. OTROSCHENKO, J. PEDERSEN, and B. RASMUSSEN, Nucl. Phys. A165(1971)449.
- [8] See, for example, J.R. STEHN, et.al., Brookhaven National Laboratory Report, BNL325, Second Edition, Supplement No.2(1965); References to specific (n,f) cross section data used in this paper are given in the analysis section where appropriate.
- [9] A.H. WAPSTRA and N.B. GOVE, Nuclear Data Tables 9, (1971)265.
- [10] M.J. MARTIN, Nuclear Data Sheets, Section B5(1971)287; M.B. LEWIS, Nuclear Data Sheets, Section B5(1971)601.
- [11] J.D. CRAMER and H.C. BRITT, Phys. Rev. C2(1970)2350; J.D. CRAMER, Los Alamos Scientific Laboratory Report, LA-4198, 1969 (unpublished).
- [12] B.B. BACK, OLE HANSEN, H.C. BRITT, J.D. GARRETT, Phys. Rev. C (to be published).
- [13] H.C. BRITT and J.D. CRAMER, Phys. Rev. C2(1970)1758.
- [14] B.B. BACK, OLE HANSEN, B. LEROUX, H.C. BRITT and J.D. GARRETT, Phys. Rev. C (to be published).
- [15] M. BOLSTERLI, L.O. FISET, J.R. NIX, and J.L. NORTON, Phys. Rev. C5(1972)1050.
- [16] C.F. TSANG, private communication; S.G. NILSSON, C.F. TSANG, A. SOBICZEWSKI, A. SZYMANSKI, S. WYCECH, C. GUSTAFSSON, I.L. LAMM, P. MOLLER, and B. NILSSON, Nucl. Phys. A131(1969)1.
- [17] F.A. RICKEY, E.T. JURNEY and H.C. BRITT, Phys. Rev. C6(1972)2072.
- [18] M.S. MOORE and G.A. KEYWORTH, Phys. Rev. C3(1971)1656.
- [19] L.G. MORETTO, Paper IAEA/SM-k74/204, this conference.
- [20] B.R. MOTTELSON, A. BOHR, S. BJØRNHOLM, Paper IAEA/SM-174/205, this conference.
- [21] N.B. GOVE and A.H. WAPSTRA, Nucl Data Tables 11(1972)127.
- [22] S. BJØRNHOLM, private communication; S. BJØRNHOLM and J.E. LYNN, Rev. Mod. Phys. (to be published).
- [23] G.D. JAMES, J.E. LYNN, and L.G. EARWAKER, Nucl. Phys. A189(1972)225.

Table I. Estimated Barriers for Odd A and Odd-Odd Nuclei. Values given in parentheses were estimated as described in text and held fixed during fitting of data. For Pa, U, and Np nuclei values for  $G_n$  and  $G_\gamma$  not in parentheses were obtained from fitting the magnitude of  $P_f$  but the values are not unique and depend also on values of some of the other parameters that were held fixed.

Nucleus	$E_A$	$E_B$	$\hbar\omega_A$	$\hbar\omega_B$	$G_n$	$G_\gamma$
$^{231}\text{Pa}$	$5.75 \pm 0.30$	$5.85 \pm 0.30$	(0.8)	(0.45)	(0.3)	3.6
$^{232}\text{Pa}$	$5.75 \pm 0.30$	$6.10 \pm 0.30$	(0.6)	(0.45)	0.45	(3.6)
$^{233}\text{Pa}$	$5.85 \pm 0.30$	$6.00 \pm 0.30$	(0.8)	(0.40)	(0.3)	1.8
$^{235}\text{U}$	$6.10 \pm 0.30$	$5.65 \pm 0.30$	(0.85)	(0.50)	(0.3)	(2.5)
$^{237}\text{U}$	$6.35 \pm 0.30$	$5.95 \pm 0.30$	(0.85)	(0.55)	0.12	(2.5)
$^{239}\text{U}$	$6.55 \pm 0.30$	$6.30 \pm 0.30$	(0.90)	(0.65)	0.05	(2.5)
$^{234}\text{Np}$	$5.35 \pm 0.30$	$5.00 \pm 0.30$	(0.6)	(0.42)	(0.3)	2.6
$^{235}\text{Np}$	$5.60 \pm 0.30$	$5.20 \pm 0.30$	(0.8)	(0.55)	(0.3)	3.6
$^{236}\text{Np}$	$5.70 \pm 0.30$	$5.20 \pm 0.30$	(0.6)	(0.42)	(0.3)	2.5
$^{237}\text{Np}$	$5.70 \pm 0.30$	$5.50 \pm 0.30$	(0.8)	(0.55)	(0.3)	2.8
$^{238}\text{Np}$	$6.00 \pm 0.30$	$6.00 \pm 0.30$	(0.6)	(0.42)	.04	(1.8)
$^{239}\text{Np}$	$5.85 \pm 0.30$	$5.50 \pm 0.30$	(0.8)	(0.55)	(0.3)	1.8
$^{239}\text{Pu}$	$6.43 \pm 0.20$	(5.50)	$1.00 \pm 0.10$	(0.55)	$0.30 \pm 0.15$	$0.77 \pm 0.12$
$^{241}\text{Pu}$	$6.25 \pm 0.20$	(5.50)	$1.10 \pm 0.10$	(0.55)	$0.30 \pm 0.15$	$1.15 \pm 0.40$
$^{243}\text{Pu}$	$6.05 \pm 0.20$	(5.60)	$0.80 \pm 0.10$	(0.55)	$0.15 \pm 0.08$	(1.2)
$^{245}\text{Pu}$	$5.72 \pm 0.20$	(5.45)	$0.90 \pm 0.10$	(0.55)	$0.40 \pm 0.15$	(1.2)
$^{240}\text{Am}$	$6.35 \pm 0.20$	(4.80)	$0.60 \pm 0.10$	(0.42)	$0.70 \pm .20$	(1.2)
$^{241}\text{Am}$	$6.00 \pm 0.20$	(4.80)	$0.80 \pm 0.10$	(0.55)	(0.3)	$1.8 \pm 0.9$
$^{242}\text{Am}$	$6.38 \pm 0.20$	(4.80)	$0.50 \pm 0.10$	(0.42)	$0.08 \pm .05$	(1.2)
$^{243}\text{Am}$	$5.98 \pm 0.20$	(4.80)	$0.75 \pm 0.10$	(0.55)	(0.3)	$1.8 \pm 0.9$
$^{244}\text{Am}$	$6.18 \pm 0.20$	(4.80)	$0.50 \pm 0.10$	(0.42)	$0.15 \pm .07$	(1.2)
$^{245}\text{Am}$	$5.88 \pm 0.20$	(4.80)	$0.85 \pm 0.10$	(0.55)	(0.3)	$1.8 \pm 1.0$
$^{247}\text{Am}$	$5.60 \pm 0.20$	(4.80)	$0.90 \pm 0.10$	(0.55)	(0.3)	$1.8 \pm_{1.8}^4$
$^{245}\text{Cm}$	$6.38 \pm 0.20$	(4.20)	$0.65 \pm 0.10$	(0.55)	$0.20 \pm 0.13$	(0.4)
$^{247}\text{Cm}$	$6.20 \pm 0.20$	(4.20)	$0.70 \pm 0.10$	(0.55)	$0.20 \pm 0.10$	(0.4)
$^{249}\text{Cm}$	$5.80 \pm 0.20$	(4.20)	$0.75 \pm 0.10$	(0.55)	$0.15 \pm 0.08$	$0.38 \pm 0.12$
$^{249}\text{Bk}$	$6.05 \pm 0.20$	(4.20)	$0.80 \pm 0.10$	(0.55)	(0.3)	$1.8 \pm .65$

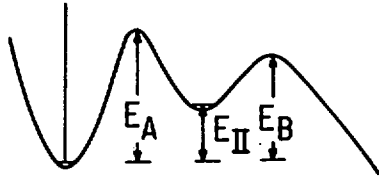
## FIGURE CAPTIONS

- Fig.1 Schematic illustration of the major features of the direct reaction fission and fission isomer population processes.
- Fig.2 Actinide nuclei for which data is currently available from direct reaction fission or(n,f) cross section measurements, DRF, and fission isomer excitation functions and halflives. Heavily outlined boxes indicate nuclei that were used as targets in the present DRF studies.
- Fig.3 Schematic diagram of the experimental setup for the direct reaction fission experiments.
- Fig.4 Measured coincidence (circles) and singles (triangles) spectra for a variety of reactions. Solid lines indicate interpolated singles cross sections for the target element. Singles spectra have been normalized to the level of the accidental contributions in the coincidence spectrum.
- Fig.5 Measured coincidence (circles) and singles (triangles) spectra for a variety of reactions. Solid lines indicate interpolated singles cross sections for the target element. Singles spectra have been normalized to the level of the accidental contributions in the coincidence spectrum.
- Fig.6 A schematic illustration of the statistical model used to fit the experimental fission probability distribution.
- Fig.7 Calculations of the total level density as a function of excitation energy. Solid and dashed lines show results obtained using the saddle point integration method. Open and closed triangles show estimates of the total density of discrete levels from the single particle spectra of Bolsterli et.al.(Ref.15) and Tsang (Ref.16), respectively.
- Fig.8 Calculations of the total level density using the saddle point integration method (solid line) compared with calculated discrete levels from Bolsterli et.al. (Ref.15) and the experimentally observed levels of Rickey et.al.(Ref.17).
- Fig.9 Fission probabilities for Am and Bk nuclei. Solid curves indicate best fits with the statistical model described in the text. Data for  $^{242}\text{Am}$  and  $^{244}\text{Am}$  were taken from Back et.al.(Ref.7).
- Fig.10 Fission probabilities for Pu and Cm nuclei. Solid curves indicate best fits with the statistical model described in the text. Data for  $^{239}\text{Pu}$  were taken from Back et.al.(Ref.7) and (n,f) data were taken from Auchampaugh et.al.(Ref.6) and Moore and Keyworth (Ref.18).
- Fig.11 Fission probabilities for Pa and Np isotopes. Solid curves indicate best fits with the statistical model described in the text.

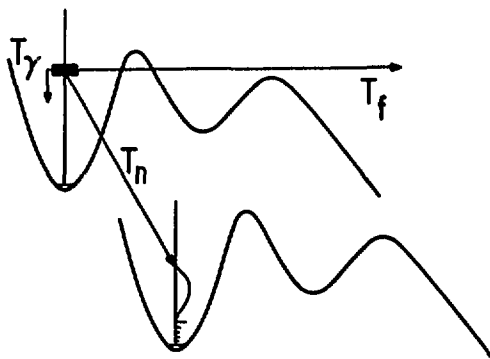
- Fig.12 Factors  $G_n$  and  $G_\gamma$  obtained from fits to the fission probabilities for Pu-Bk nuclei.
- Fig.13 Heights of the fission barriers for Pu-Bk nuclei obtained from fits to experimental fission probabilities.
- Fig.14 Heights of the fission barriers for Th-Np nuclei obtained from fits to experimental fission probabilities.



NOTATION



DIRECT REACTION FISSION

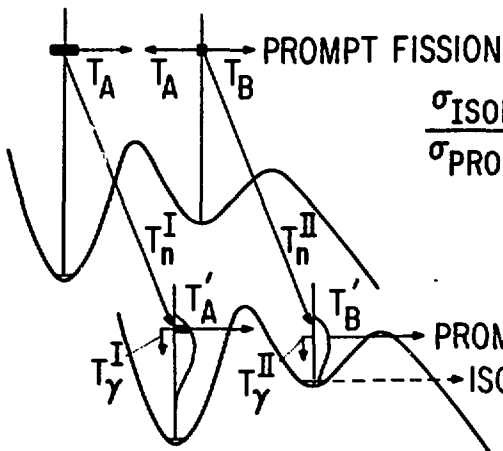


$$P_f = \left\langle \frac{T_f}{T_f + T_n + T_\gamma} \right\rangle$$

$$T_f = f(T_A, T_B)$$

$$T_f = f'(E_A, \hbar\omega_A, E_B, \hbar\omega_B)$$

FISSION ISOMER  $E^*$  FUNCTIONS



$$\frac{\sigma_{\text{ISOMER}}}{\sigma_{\text{PROMPT}}} \approx f(T_B, T_n^{II}, T_B', T_\gamma^{II}) \cdot g(T_A, T_A', T_n^I, T_\gamma^I) \approx f'(E_B, E_B', E_{II}') \cdot g$$

Fig.1 Schematic illustration of the major features of the direct reaction fission and fission isomer population



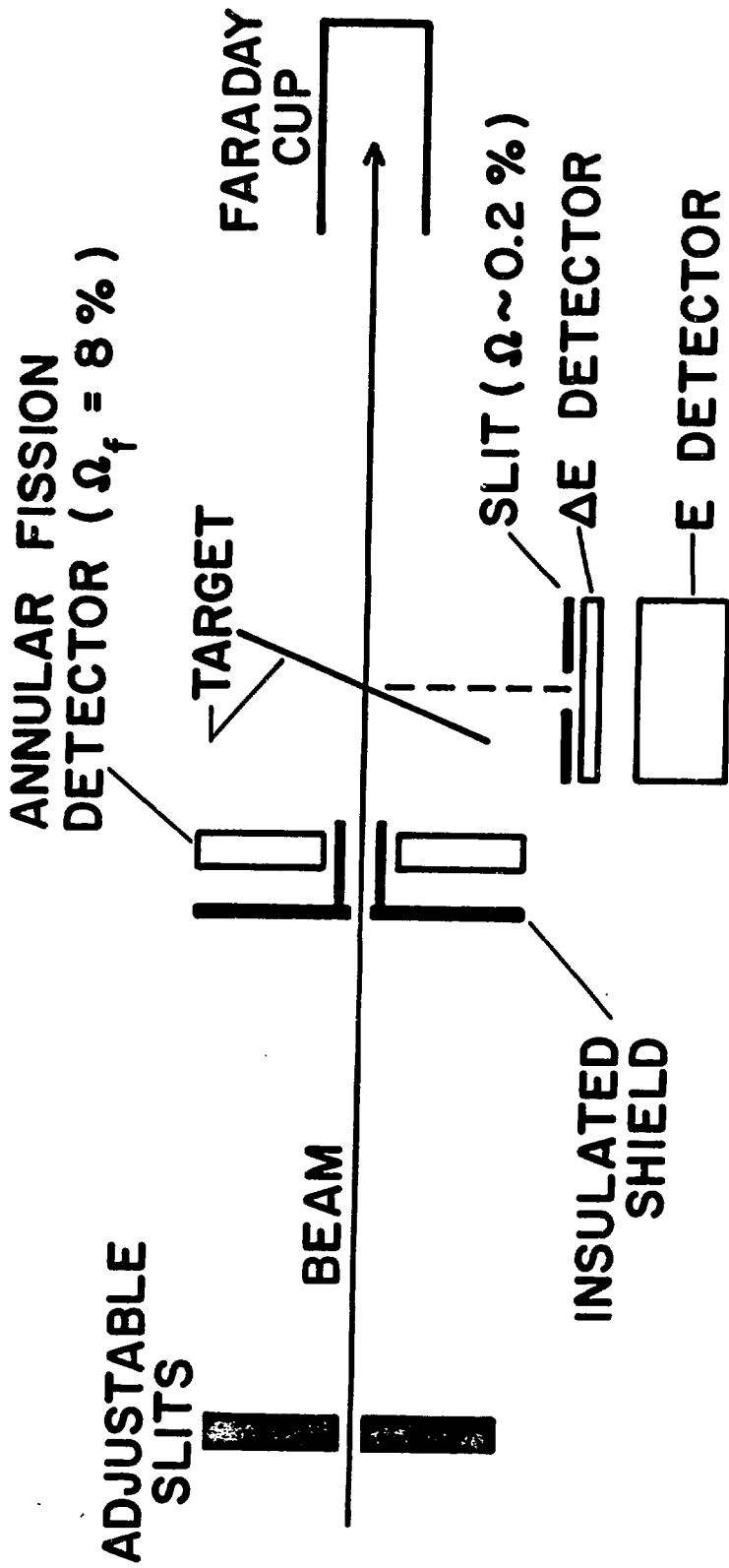


Fig.3 Schematic diagram of the experimental setup for the direct reaction fission experiments.

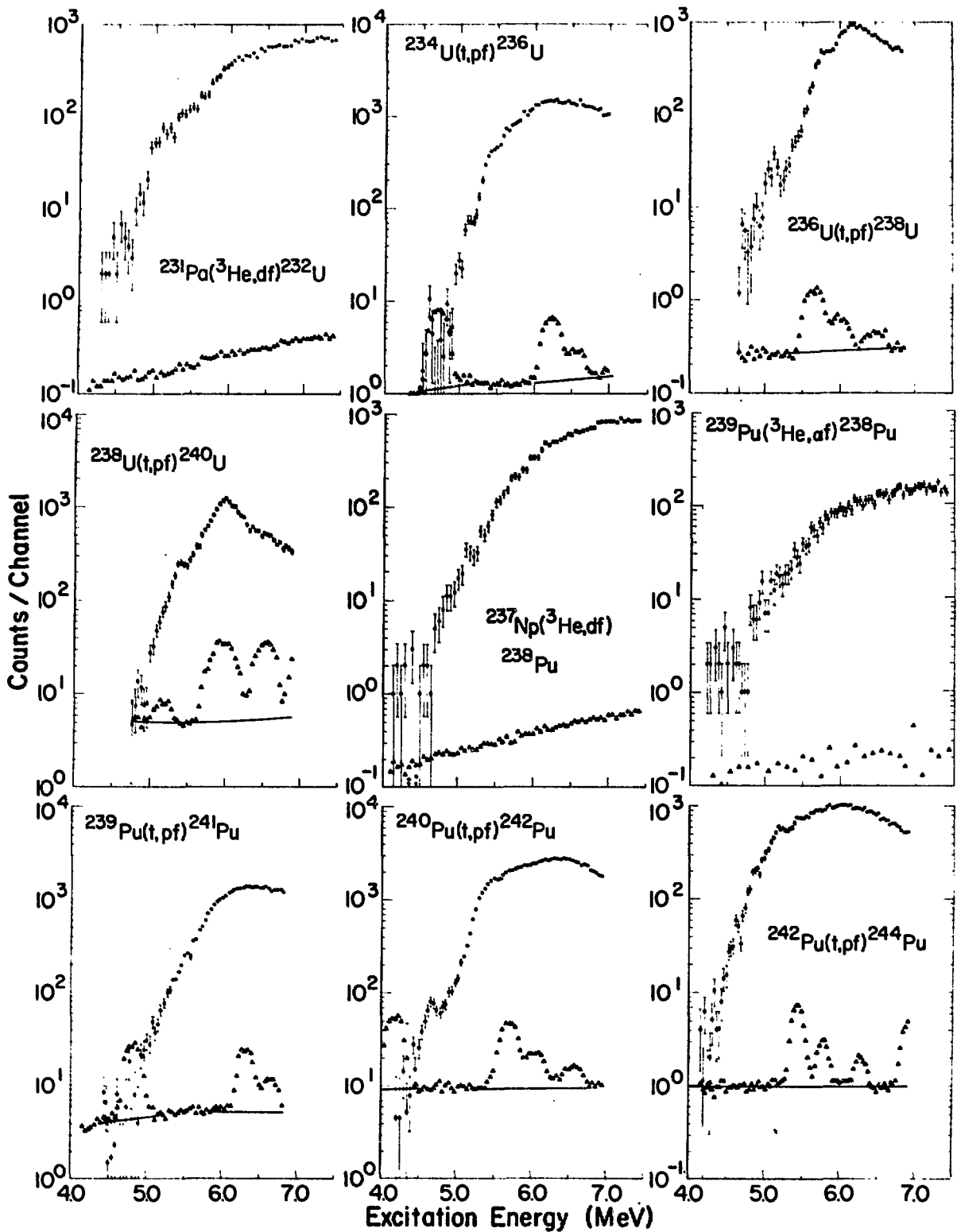


Fig.4 Measured coincidence (circles) and singles (triangles) spectra for a variety of reactions. Solid lines indicate interpolated singles cross sections for the target element. Singles spectra have been normalized to the level of the accidental contributions in the coincidence spectrum.

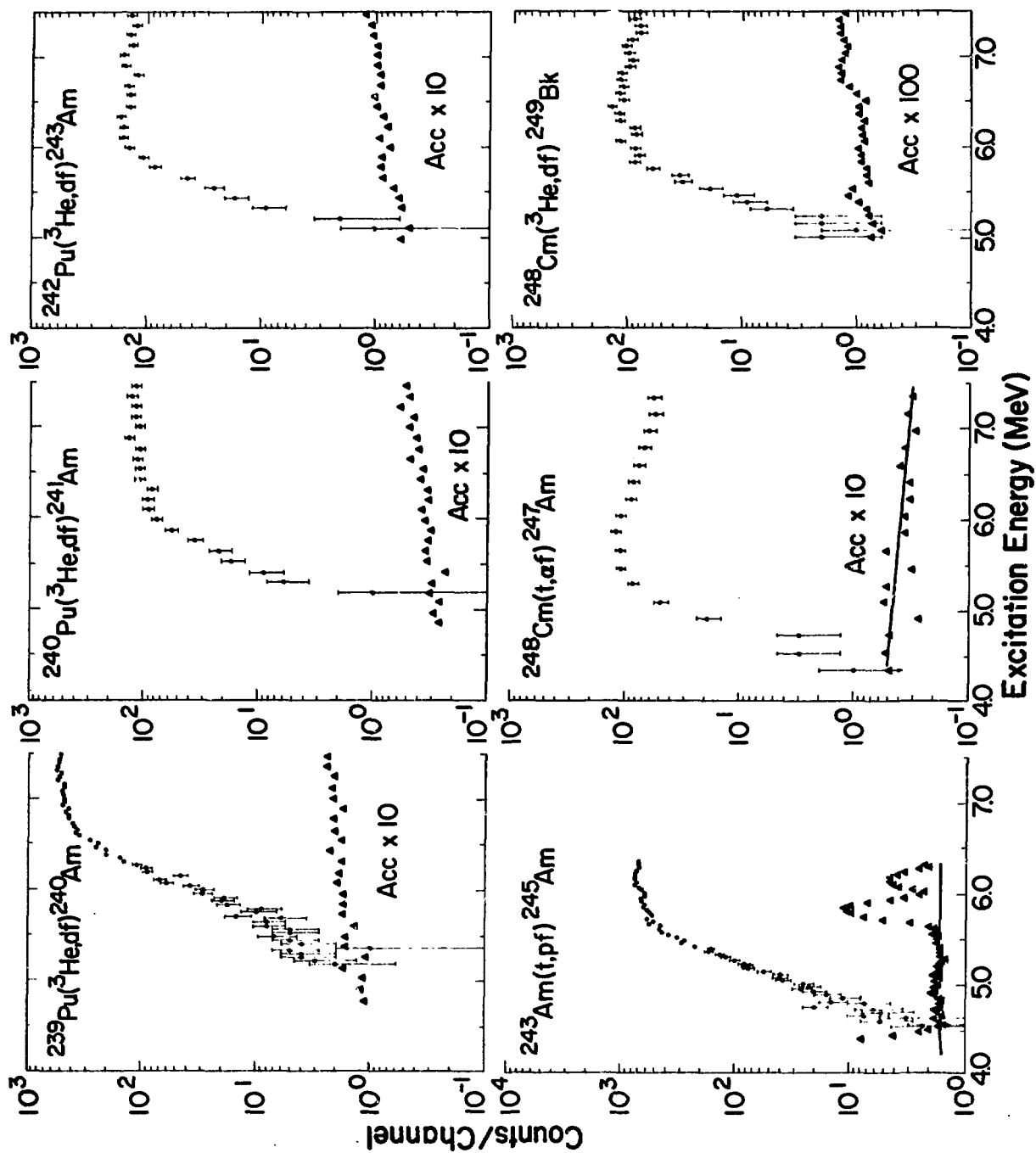


Fig. 5 Measured coincidence (circles) and singles (triangles) spectra for a variety of reactions. Solid lines indicate interpolated singles cross sections for the target element. Singles spectra have been normalized to the level of the accidental contributions in the coincidence spectrum.

# FISSION PROBABILITY IN COMPLETE DAMPING LIMIT

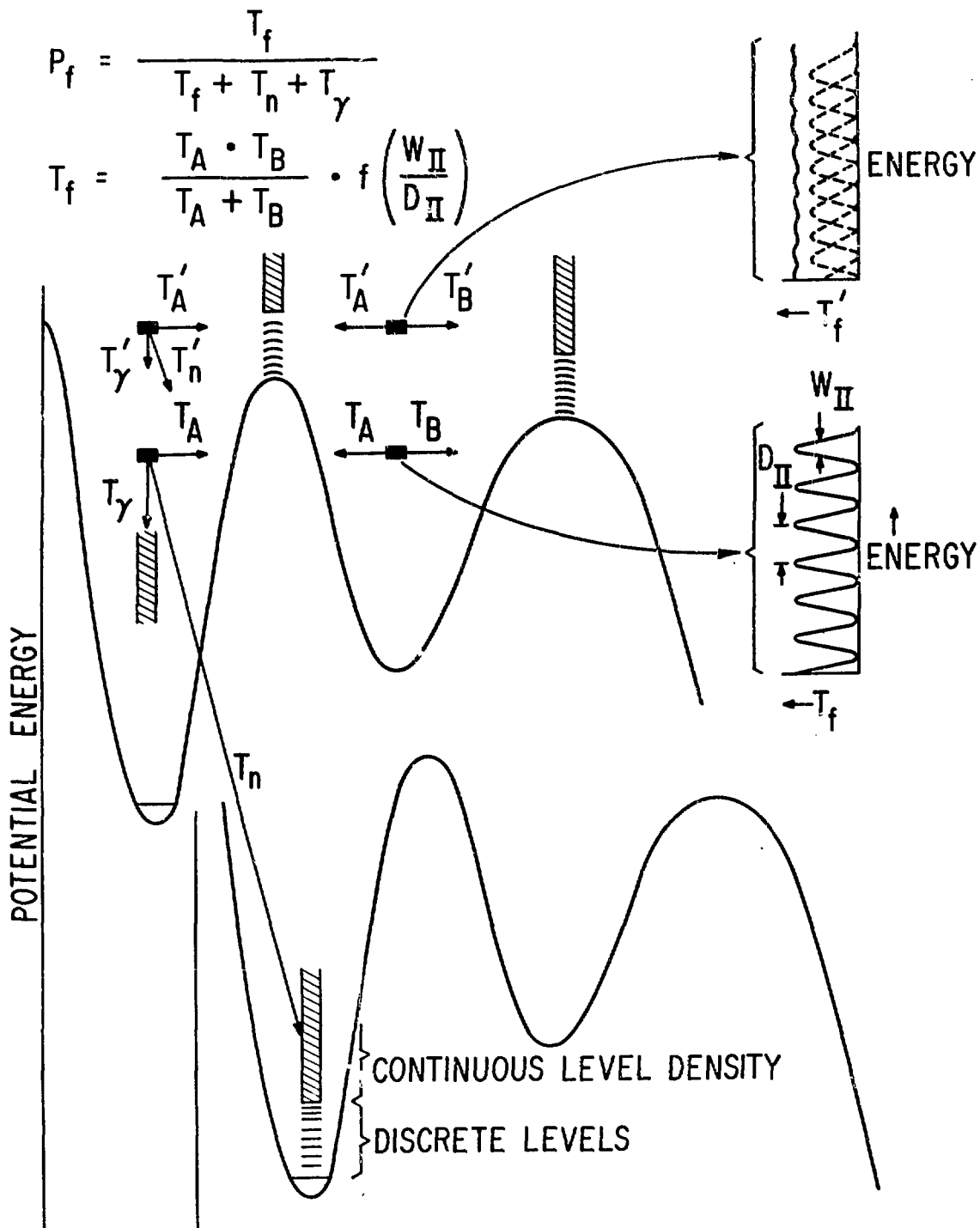


Fig.6 A schematic illustration of the statistical model used to fit the experimental fission probability distribution.

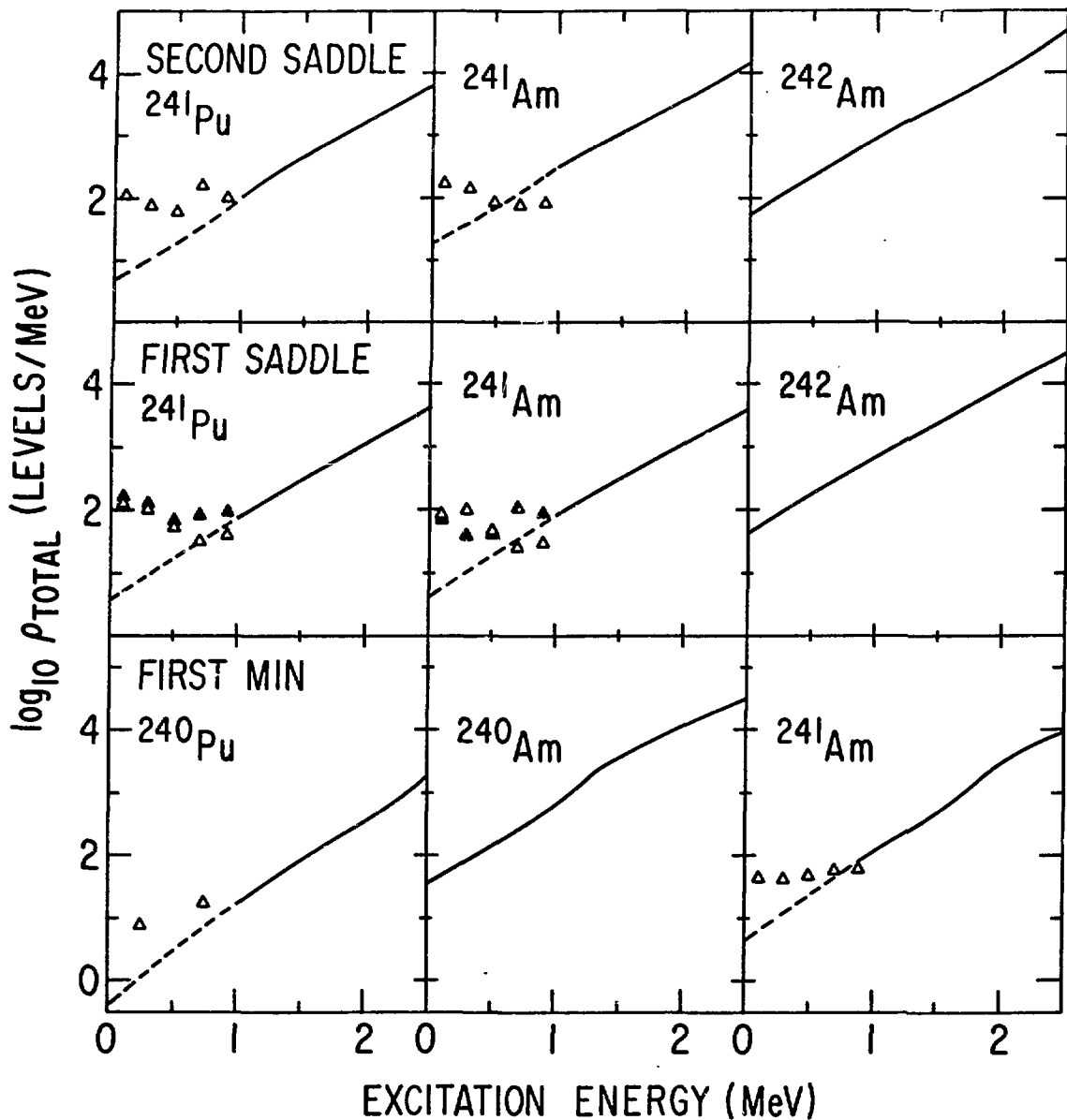


Fig.7 Calculations of the total level density as a function of excitation energy. Solid and dashed lines show results obtained using the saddle point integration method. Open and closed triangles show estimates of the total density of discrete levels from the single particle spectra of Bolsterli et.al.(Ref.15) and Tsang (Ref.16), respectively.

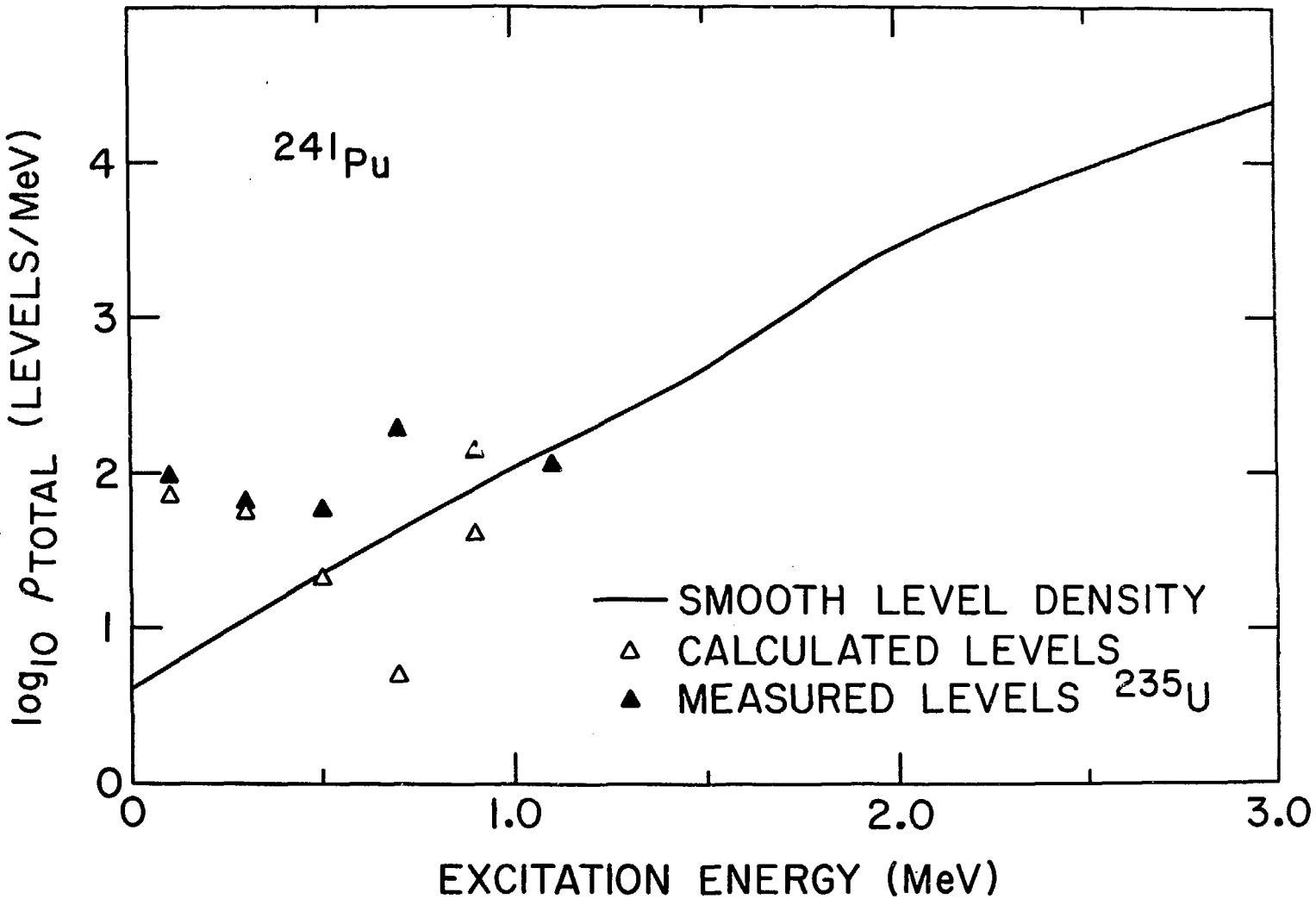


Fig. 8 Calculations of the total level density using the saddle point integration method (solid line) compared with calculated discrete levels from Bolsterli et.al. (Ref.15) and the experimentally observed levels of Rickey et.al. (Ref.17).



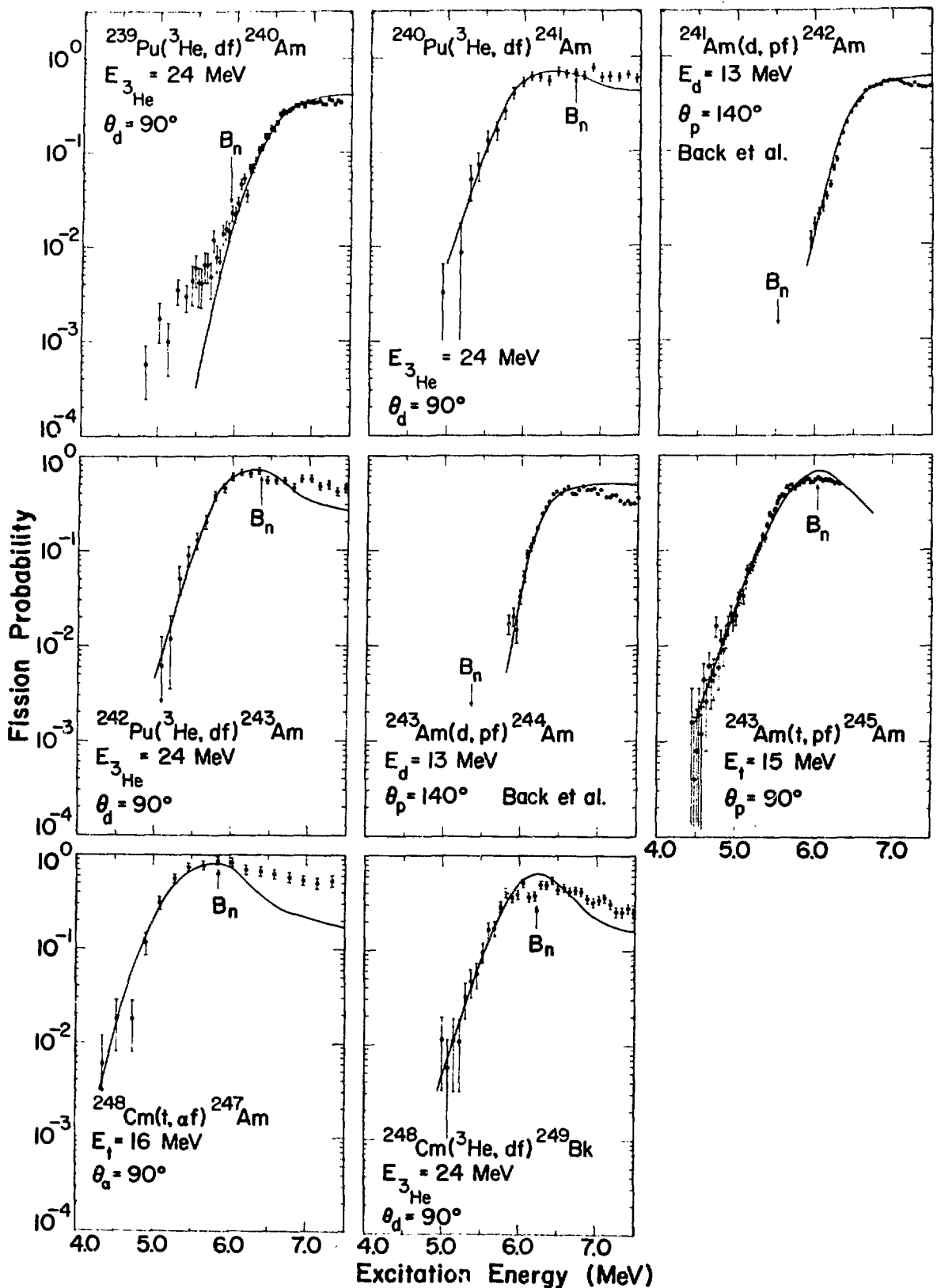


Fig.9 Fission probabilities for Am and Bk nuclei. Solid curves indicate best fits with the statistical model described in the text. Data for  $^{242}\text{Am}$  and  $^{244}\text{Am}$  were taken from Back et.al.(Ref.7).

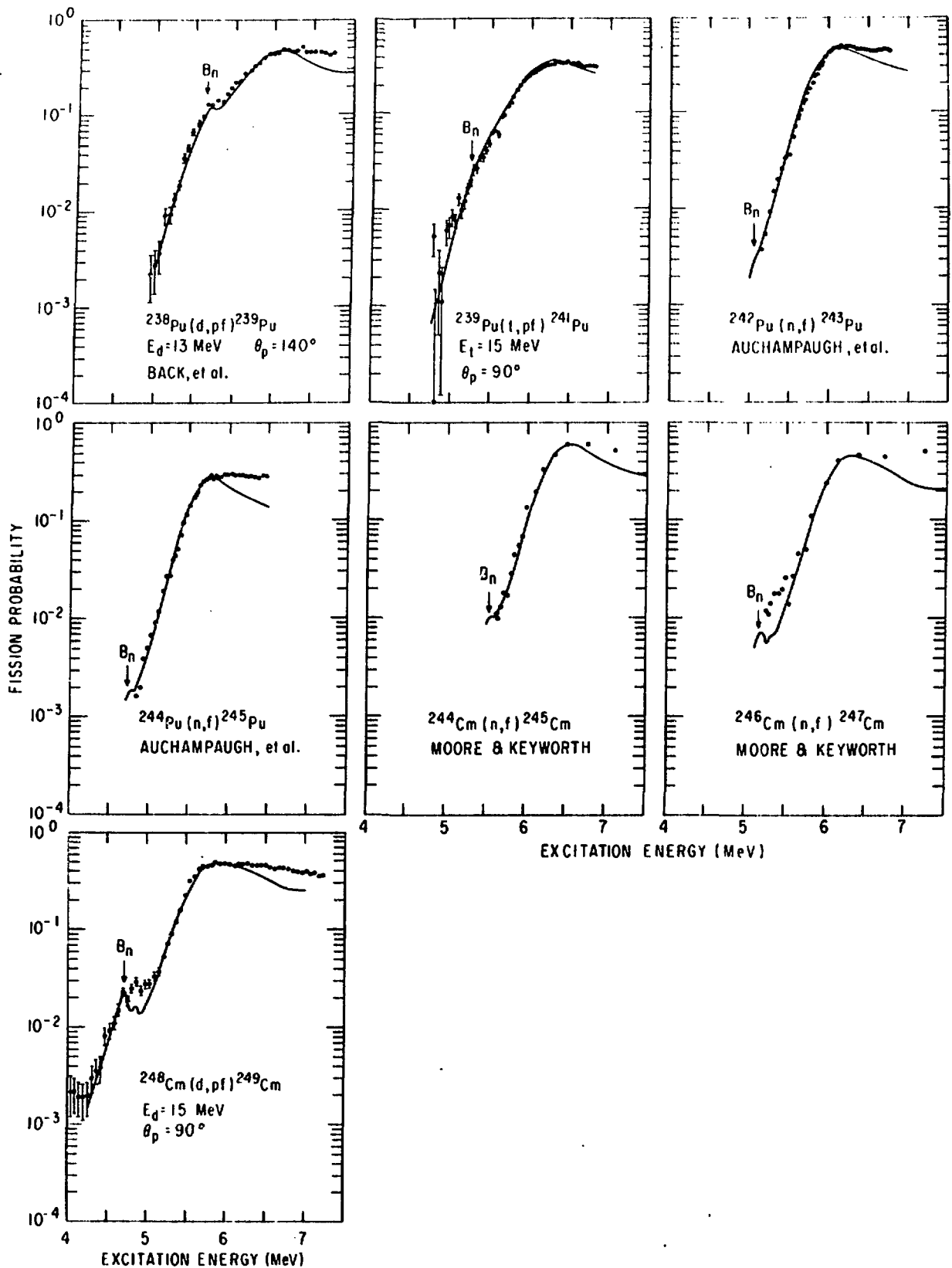


Fig.10 Fission probabilities for Pu and Cm nuclei. Solid curves indicate best fits with the statistical model described in the text. Data for  $^{239}\text{Pu}$  were taken from Back et.al.(Ref.7) and (n,f) data were taken from Auchampaugh et.al.(Ref.6) and Moore and Keyworth (Ref.18).

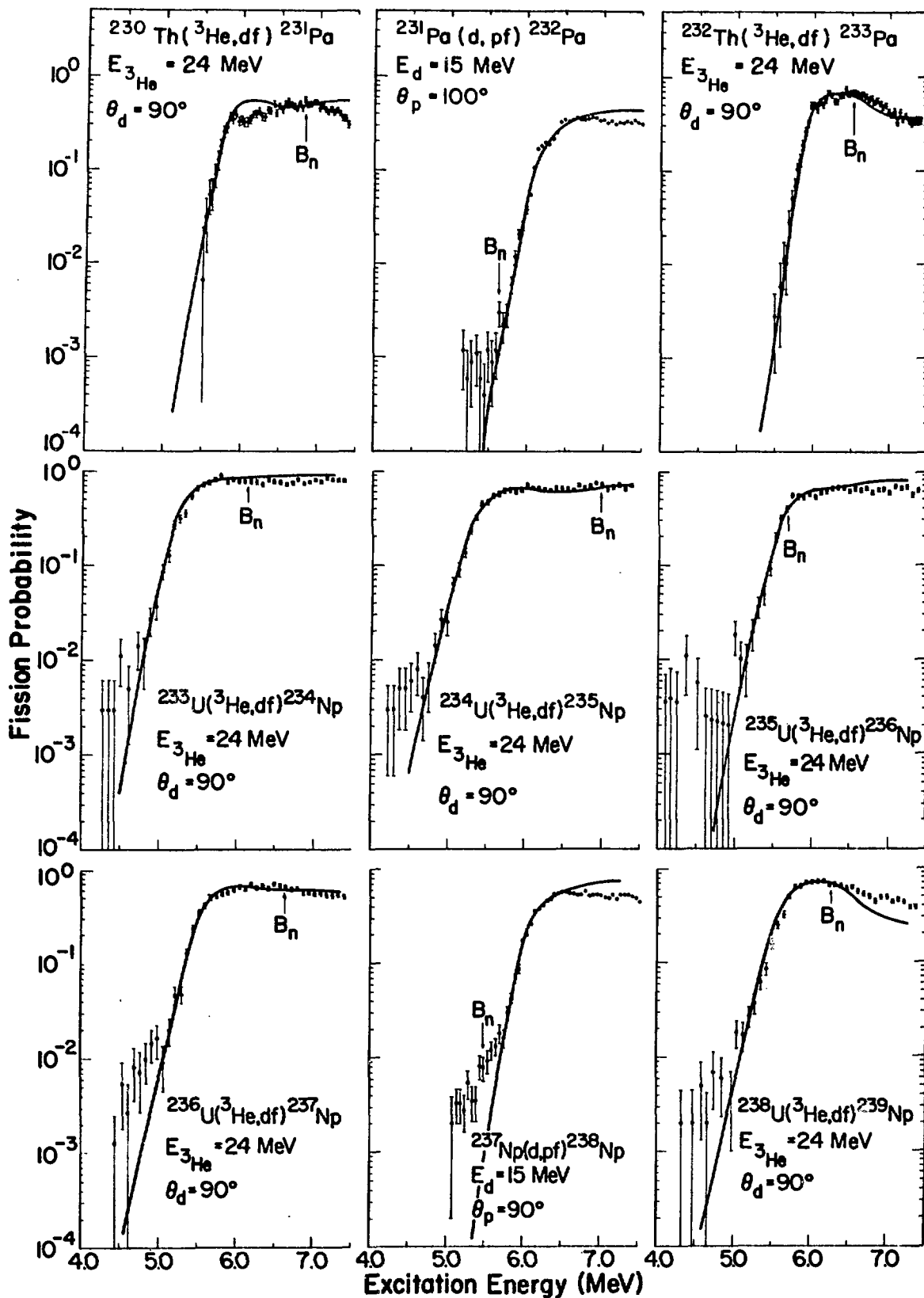


Fig.11 Fission probabilities for Pa and Np isotopes. Solid curves indicate best fits with the statistical model described in the text.

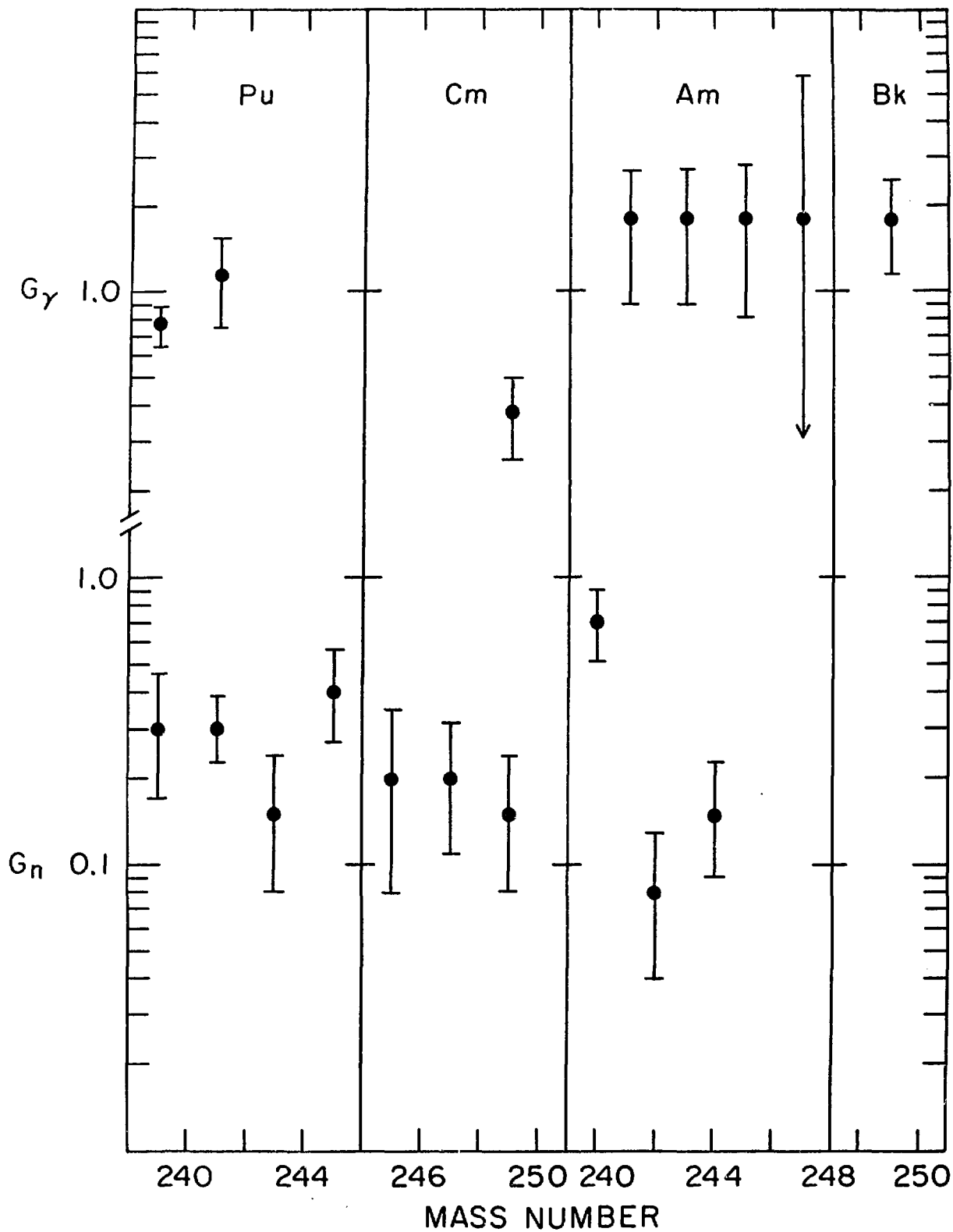


Fig.12 Factors  $G_n$  and  $G_\gamma$  obtained from fits to the fission probabilities for Pu-Bk nuclei.

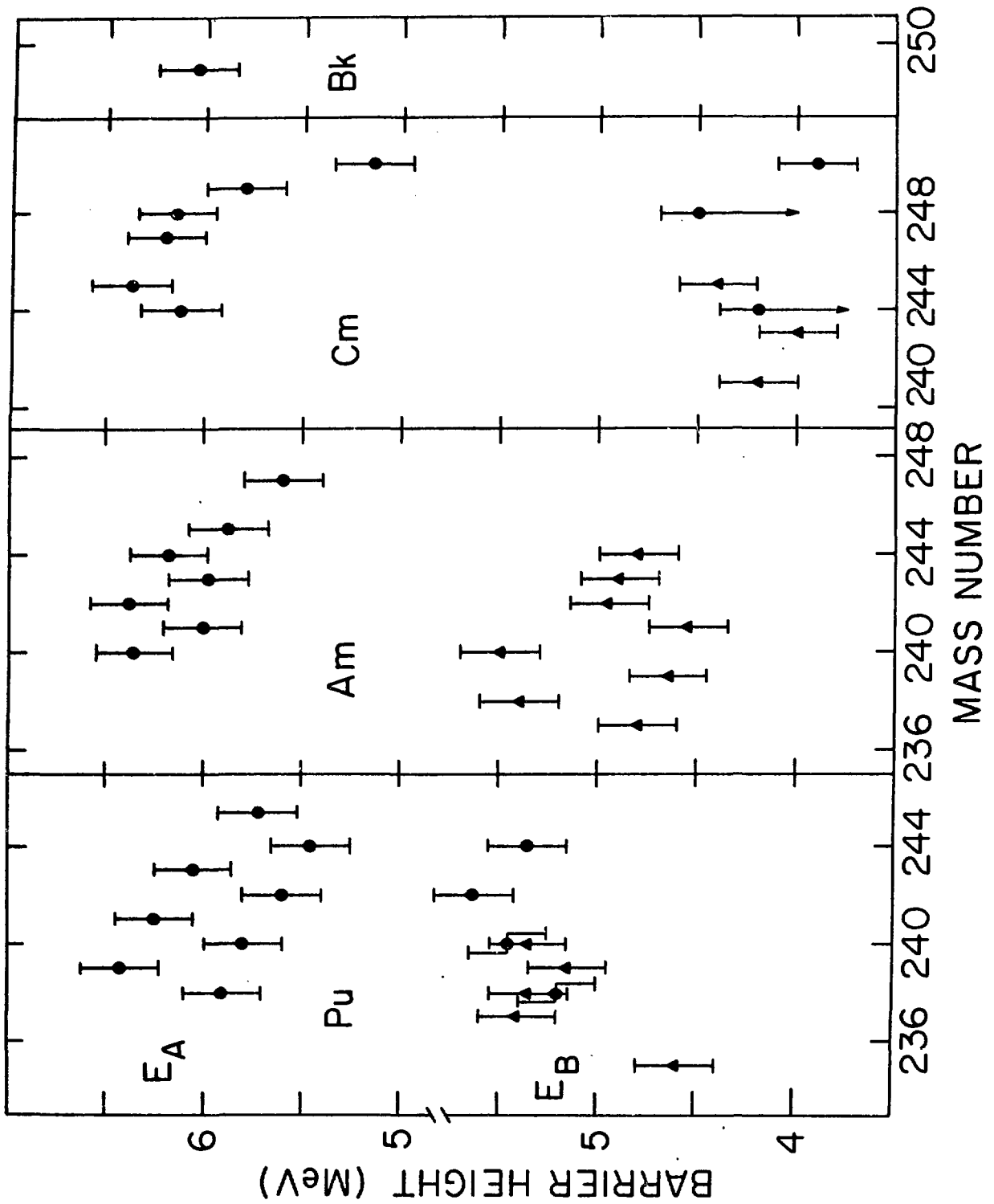


Fig.13 Heights of the fission barriers for Pu-Bk nuclei obtained from fits to experimental fission probabilities.

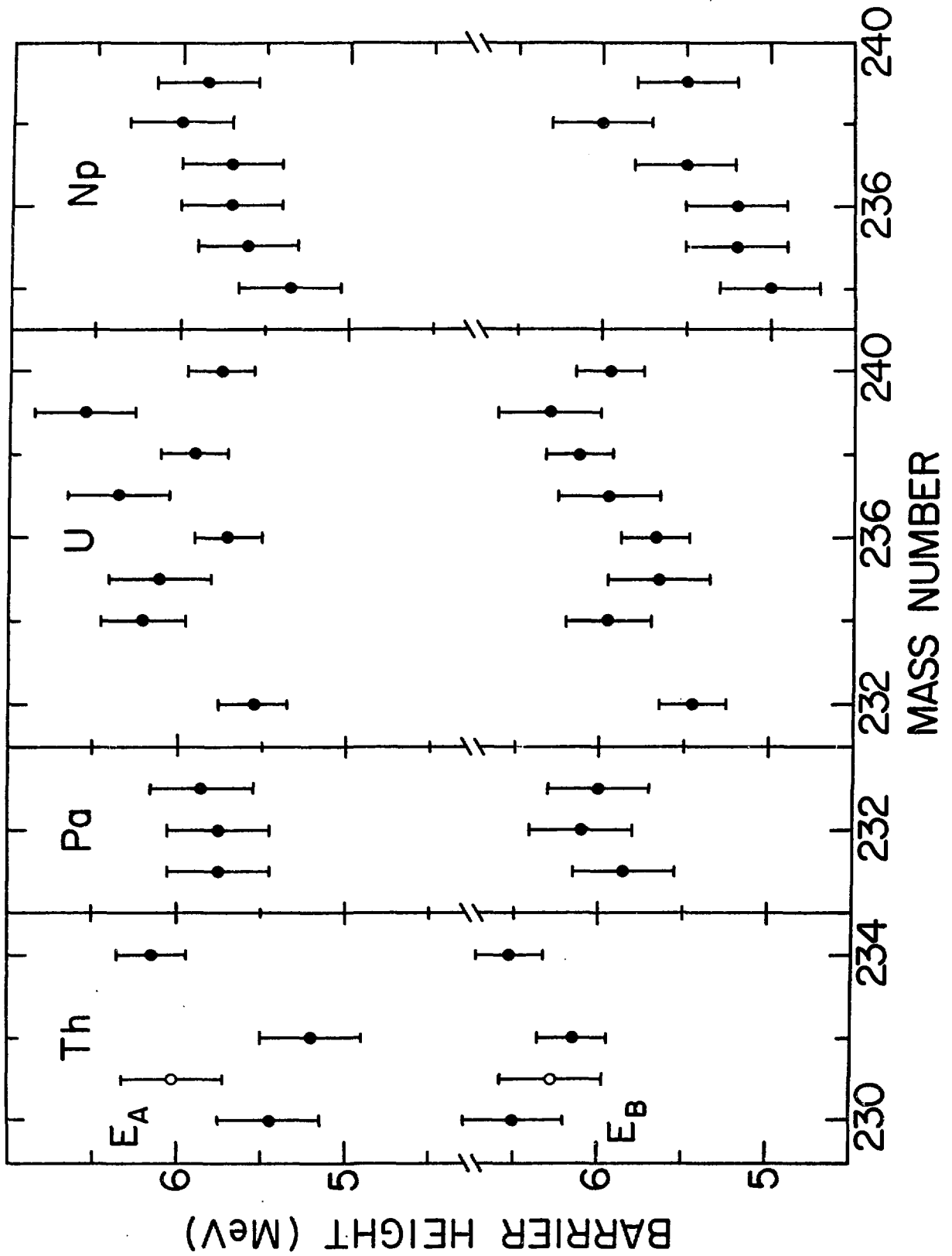


Fig.14 Heights of the fission barriers for Th-Np nuclei, obtained from fits to experimental fission probabilities.